Renormalization group analysis of macrodispersion in a directed random flow

Uwe Jaekel and Harry Vereecken[1]

Institute of Chemistry and Dynamics of the Geosphere, Research Center Jülich, Jülich, Germany

Abstract. We apply "field theoretic" methods to the calculation of the effective diffusivity (macrodispersion coefficient) in a random flow. We show how this approach can be utilized to calculate a perturbation series for the effective diffusivity of conservative tracers in an incompressible velocity field with nonvanishing mean. The first-order (i.e., "one-loop") approximation of this series coincides with classical results derived by Gelhar and Axness and Dagan. A renormalization group (RNG) approach is utilized, and the results are compared to the classical first-order perturbation theory. For a moderate variability of the permeability the renormalized theory predicts only small corrections to the longitudinal dispersivity. However, the transverse dispersivity can be larger than that predicted by the first-order perturbation theory by several orders of magnitude. We compare these values to the outcome of Monte Carlo simulations and find that the RNG predictions are in much better, though not perfect, accordance with the results of simulations. Moreover, the results are in good quantitative agreement with reported observations from the Borden Site field experiment.

1. Introduction

It is well documented in literature and known from experiments that spatial variability in the hydraulic conductivity substantially influences the transport of dissolved substances in geological media. These variations cause fluctuations in the flow velocities of water introducing an additional dispersion mechanism. This process is termed macrodispersive behavior and is described in the three-dimensional (3-D) case by a macrodispersion tensor. Large-scale tracer experiments [*Sudicky*, 1986; *LeBlanc*, 1991] have shown that because of these variations in the velocity field, the spread of the tracer plume is much larger than would be expected on the basis of column experiments. In the last years, there has been considerable interest in calculating the asymptotic values of this macrodispersion tensor with respect to time.

Gelhar and Axness [1983] used stochastic solutions of the first-order perturbed steady flow and convection-dispersion equation to calculate an effective macrodispersivity tensor. A three-dimensional statistically anisotropic exponential covariance function was used to describe the spatial dependence of the hydraulic conductivity. From their theory they found that the calculated transverse dispersivities are several orders of magnitude smaller than the longitudinal component for the isotropic case. The longitudinal dispersivity of the macrodispersivity was found to be convectively controlled depending upon the variance and covariance length of the hydraulic conductivity. For the anisotropic case they found that all components of the macrodispersivity tensor are convectively controlled. Comparing their theory with the calculated dispersivities from the Borden Site field experiment, a good agreement

was found with the longitudinal component. The calculated transverse dispersivities, however, were much smaller than the values estimated from the spatial moments.

Using a Lagrangian formulation of the transport problem in heterogeneous formations, *Dagan* [1989] obtained expressions relating the time dependent behavior of dispersion to the statistical properties of the hydraulic conductivity field. Using his theory, *Dagan* [1987] could recover the results obtained by *Gelhar and Axness* [1983] using different assumptions. For the asymptotic behavior of the transverse dispersivity with time, Dagan obtains values which tend to zero. From tracer experiments it is known that the transverse dispersivity tend to finite values different from zero.

In both approaches the basic assumptions are that the average flow is uniform, the flow domain is unbounded, and a first-order approximation in the variance of the log transformed hydraulic conductivity is used. Theories using these first-order approximations are also coined linear theories. This linear approach implies that tracer particles do not deviate from their ensemble mean trajectory which may lead to an underestimation of the transverse dispersivities.

Neuman and Zhang [1990] and *Zhang and Neuman* [1990] presented a quasi-linear theory accounting for the nonlinearity caused by deviations of the tracer particles from the mean trajectory. This was realized by introducing Corrsin's Conjecture assuming that the displacement residuals of the particles and the Fourier components of the velocity are only weakly correlated. They found good agreement with the macrodispersivity values calculated from the Borden Site tracer experiment.

In this paper we present an alternative approach based on an approximate renormalization group (RNG) analysis to calculate the effective dispersion tensor for statistically homogeneous and anisotropic hydraulic conductivity fields. The basic idea of this method is to calculate averaged concentrations not by a perturbation theory for the whole field in one single step but by averaging step by step over bands of wave numbers, starting at high wave numbers (i.e., performing a small-scale

---

[1]Now at Institute of Petroleum and Organic Geochemistry, Forschungszentrum Julich GmbH, Julich, Germany.

average) until all fluctuations have been "averaged out." This leads to a scale dependent dispersion coefficient.

Feynman [1948] was the first to represent a formal perturbation series by diagrams. This type of representation is coined Feynman diagrams and is widely used in statistical thermodynamics, many body problems, and quantum electrodynamics. The first application of diagrammatic methods on transport in random flow was made by *Kraichnan* [1961]. *Phythian and Curtis* [1978] used renormalized perturbation series and diagrammatic analysis to characterize effective diffusivity in a Gaussian random flow field. *King* [1987] introduced diagrammatic analysis to represent an infinite series of the stochastic pressure equation in heterogeneous porous media. From this representation, King obtained the effective permeability of the medium (including higher-order terms), the mean pressure head, and the pressure covariance. *Christakos et al.* [1995] introduced diagrammatic analysis in problems of groundwater flow in heterogeneous porous formations. For a 3-D flow problem in an isotropic bounded domain with Dirichlet boundary conditions an integral equation for the mean hydraulic head was derived. They found good agreement between the numerical performance of the diagrammatic approach and the exact solutions of one-dimensional (1-D) stochastic flow examples. *Zhang* [1995] used a diagrammatic analysis and RNG expansions to analyze Corrsin's hypothesis which is used to obtain closed form equations for the equation governing the second moment of particle displacement fluctuations in a random field. Zhang showed that this hypothesis represents the leading term contribution in a RNG perturbation expansion.

RNG methods were originally developed [*Wilson and Kogut*, 1974] for problems in quantum field theory and many body problems. These methods were first applied by *Yakhot and Orszag* [1986] on turbulent transport, and a huge number of further applications on transport in random media were then found [e.g., *Bouchaud and Georges*, 1990]. *Avellaneda and Majda* [1992a, b] constructed an exact RNG method for a special case of diffusion in a random velocity field (and showed that the approximate RNG analysis may fail in predicting the correct scaling law for anomalous diffusion).

Usually, RNG methods are applied in cases where naive perturbation theory would yield divergent results, for example, for the Eulerian formulation of the well-known case of transport in a stratified aquifer discussed by *Matheron and de Marsily* [1980] which is covered by *Avellaneda and Majda* [1992a, b]. However, approximate RNG methods can often give very good, sometimes exact, results [e.g., *Dean et al.*, 1994; *Deem and Chandler*, 1994] in cases where naive perturbation theory predicts finite values but where its applicability is questionable because of the strength of the perturbations.

The purpose of the present paper is therefore to perform an approximate RNG analysis for the cases studied by *Gelhar and Axness* [1983]. The calculated values are compared with classical results and observations obtained from the Borden Site experiment.

The organization of this paper is as follows: In section 2 we formulate a formal perturbation expansion with a diagrammatic method. In section 3 we show how the macrodispersion coefficient can be obtained from the sum over connected diagrams and that this expansion recovers in its lowest order the classical result derived by *Gelhar and Axness* [1983]. Using an iterative averaging procedure, in section 4 we formulate a renormalization group analysis for this problem, leading to a system of ordinary differential equations whose numerical so-

lutions are sketched in section 5. In section 6, in order to check the validity of our analysis we compare the results to the outcome of some Monte Carlo simulations. In section 7 we present a first application to field data from the Borden Site. Finally, in section 8 we present a summary and conclusions of our results.

2. Perturbation Theory

Our starting point is the convection dispersion equation

$$\frac{\partial c}{\partial t} + \mathbf{v} \cdot \nabla c = D_{lm} \frac{\partial^2}{\partial x_l \partial x_m} c \qquad (1)$$

with a local dispersion tensor D_{lm} which we assume to be constant for simplicity. We assume that the velocity field can be decomposed into a homogeneous field $\mathbf{U}$ and a stochastic component $\mathbf{u}$ with zero mean

$$\mathbf{v}(\mathbf{x}) = \mathbf{U} + \mathbf{u}(\mathbf{x})$$
$$\langle \mathbf{v}(\mathbf{x}) \rangle = \mathbf{U} \equiv \text{const} \qquad (2)$$

We further assume that the field $\mathbf{u}$ is statistically homogeneous, that is, the (ensemble-averaged) covariance functions of the field at different positions depend only on the distance vector of the positions (dependance only on the distance would additionally imply isotropy)

$$\langle u_l(\mathbf{x}) u_m(\mathbf{x}') \rangle = \Delta_{lm}(\mathbf{x} - \mathbf{x}') \qquad (3)$$

Fourier transforming this equation yields

$$\langle \hat{u}_l(\mathbf{k}) \hat{u}_m(\mathbf{k}') \rangle = (2\pi)^d \hat{\Delta}_{lm}(\mathbf{k}) \delta(\mathbf{k} + \mathbf{k}') \qquad (4)$$

where $\hat{f}$ means the Fourier transform of the function f and δ denotes the D-dimensional Dirac distribution.

2.1. Feynman Rules

In this section we derive the Feynman rules for the calculation of the ensemble-averaged Green's function of the transport equation (equation (1)) which allow us to write down the contributions of arbitrary orders to a formal perturbation theory. The Green's function $G(\mathbf{x}, t; \mathbf{x}', t')$ can be defined as the solution of the transport equation with a point source term at time t' and position $\mathbf{x}'$. For notational convenience we set $t' = 0$ and $\mathbf{x}' = 0$ such that

$$\frac{\partial}{\partial t} G(\mathbf{x}, t) + [\mathbf{U} + \mathbf{u}(\mathbf{x})] \cdot \nabla G(\mathbf{x}, t) - D_{lm} \frac{\partial^2}{\partial x_l \partial x_m} G(\mathbf{x}, t)$$
$$= \delta(\mathbf{x}) \delta(t) \qquad (5)$$

Now we denote by $\hat{G}(\mathbf{k}, \omega)$ the Fourier transform of G with respect to the spatial coordinates and the time. Therefore

$$G(\mathbf{x}, t) = \frac{1}{(2\pi)^{d+1}} \int d^d k \int d\omega \, \hat{G}(\mathbf{k}, \omega)$$
$$\cdot \exp[i(\mathbf{k} \cdot \mathbf{x} + \omega t)] \qquad (6)$$

plugging this into (5), we obtain

$$i\omega \hat{G}(\mathbf{k}, \omega) + i\mathbf{U} \cdot \mathbf{k} \hat{G}(\mathbf{k}, \omega) + D_{lm} k_l k_m \hat{G}(\mathbf{k}, \omega)$$
$$= 1 - \frac{i}{(2\pi)^d} \int d^d q \, \hat{\mathbf{u}}(\mathbf{q}) \cdot (\mathbf{k} - \mathbf{q}) \hat{G}(\mathbf{k} - \mathbf{q}, \omega) \qquad (7)$$

which can be rewritten as a "fixed point equation" (a fixed

point x^* of a function f is defined as a solution of the equation $x^* = f(x^*)$) for the function $\hat{G}$

$$\hat{G}(k, \omega) = \hat{G}_0(k, \omega) - \hat{G}_0(k, \omega) \frac{i}{(2\pi)^d}$$

$$\cdot \int d^d q \, \hat{u}(q) \cdot (k - q) \hat{G}(k - q, \omega) \qquad (8)$$

where $\hat{G}_0$ is defined by

$$\hat{G}_0(k, \omega) := \frac{1}{i\omega + ik \cdot U + D_{lm} k_l k_m} \qquad (9)$$

In the unperturbed case, i.e., if $u(x) = 0$, we see from (8) that $\hat{G} = \hat{G}_0$. Therefore $\hat{G}_0$ is the Green's function of the unperturbed problem.

At this point it is helpful to rewrite (8) in terms of so-called "Feynman diagrams" which are excellent bookkeeping devices for higher orders of perturbation theory. Then (8) reads

$$\rule{2cm}{1pt} = \rule{1.5cm}{0.4pt} + \rule{1.5cm}{1pt}\!\!\!\!\!\!\!\!\!\overset{\scriptstyle q}{|} \qquad (10)$$
$$\text{k} \qquad\qquad \text{k} \qquad\qquad \text{k} \quad \text{k-q}$$

The diagram has to be evaluated by the following "Feynman rules."

1. Each bold line represents a factor equal to the Green's function $\hat{G}$; a thin line represents the unperturbed Green's function $\hat{G}_0$; and a dashed line is a symbol for the l component of the perturbation $\hat{u}_l$. Each function has to be evaluated at the wave number by which it is labeled.

2. A vertex of full and dashed lines carries a factor equal to $[-i/(2\pi)^d](k - q)_l$.

3. Diagrams containing dashed lines are integrated over all wave vectors q and summed over all components l.

Now we replace the bold line on the right-hand side by the right-hand side of the diagram equation again:

$$\rule{2cm}{1pt} = \rule{1.2cm}{0.4pt} + \rule{1.2cm}{1pt}\overset{q}{|} + \rule{1.5cm}{1pt}\overset{q\;\;q'}{|\;\;|} \qquad (11)$$
$$\text{k} \qquad\quad \text{k} \qquad \text{k} \;\; \text{k-q} \qquad \text{k} \;\; \text{k-q} \;\; \text{k-q-q'}$$

We see that at a vertex the wave numbers of the dashed line q and the wave number of the dashed line at the right-hand side of the vertex $(k - q)$ sum up to the value at the left-hand side, i.e., k. Therefore all wave numbers are determined uniquely by the wave number lying at the left edge of a diagram (i.e., k in the preceeding diagram), and we can omit the labels in the diagrams. Iterating this process, one obtains an infinite series of Feynman diagrams:

$$\rule{2cm}{1.5pt} = \rule{1.5cm}{0.4pt} + \rule{1.5cm}{0.4pt} + \rule{1.5cm}{0.4pt}$$
$$+ \rule{1.5cm}{0.4pt} + \rule{1.5cm}{0.4pt} + \cdots \qquad (12)$$

Note that the Green's functions on the right-hand side are only unperturbed ones, such that we have at least formally obtained a representation of the full Green's function $\hat{G}$ in terms of $\hat{G}_0$ and $\hat{u}$. The first term in this expansion is of zeroth order in the perturbation $\hat{u}$; the second one is of first order, etc.

2.2. Ensemble Averages

Now we want to derive a series for the ensemble-averaged Green's function

$$\hat{\mathcal{G}}(k, \omega) = \langle \hat{G}(k, \omega) \rangle \qquad (13)$$

This can be done by averaging both sides of the diagrammatic perturbation series of (12). Because of the Feynman rules, this means that we have to evaluate higher-order covariance functions

$$\hat{A}^N_{l_1 l_2 \cdots l_N}(k_1, k_2, \cdots, k_N) := \langle u_{l_1}(k_1) u_{l_2}(k_2) \cdots u_{l_N}(k_N) \rangle \qquad (14)$$

Provided that the statistics of the perturbing field $u(k)$ are Gaussian with a vanishing mean, these covariance functions can be determined by the following rules: (1) Any covariance function with an odd number of arguments is zero, and (2) the covariance functions with an even number of arguments are the products of two-point covariance functions $\hat{A}^2(k_l, k'_m)$, summed over all possible pairings of the arguments. Using the homogeneity condition (4), we see that for instance the four-point covariance function of the $\hat{u}$ can be expressed as

$$\hat{A}^4_{l_1 l_2 l_3 l_4}(k_1, k_2, k_3, k_4) = \hat{A}_{l_1 l_2}(k_1) \delta(k_1 + k_2) \hat{A}_{l_3 l_4}(k_3) \delta(k_3 + k_4)$$

$$+ \hat{A}_{l_1 l_3}(k_1) \delta(k_1 + k_3) \hat{A}_{l_2 l_4}(k_2) \delta(k_2 + k_4)$$

$$+ \hat{A}_{l_1 l_4}(k_1) \delta(k_1 + k_4) \hat{A}_{l_2 l_3}(k_2) \delta(k_2 + k_3) \qquad (15)$$

This averaging process can be symbolized diagrammatically by combining all possible pairs of dashed lines to loops, i.e., to the fourth order

$$\rule{2cm}{1.5pt} = \rule{1.2cm}{0.4pt} + \underset{2}{\overset{\frown}{\rule{1.2cm}{0.4pt}}} +$$
$$+ \underset{3}{\rule{1.2cm}{0.4pt}} + \underset{4}{\rule{1.2cm}{0.4pt}} + \underset{5}{\rule{1.2cm}{0.4pt}} + \cdots \qquad (16)$$

where the heavy line on the left-hand side now denotes the averaged Green's function.

Let us now cut the "external" lines in the Feynman diagrams before the first and behind the last vertex by dividing the corresponding expression by $G_0(k)^2$ and define such truncated diagrams as connected if they cannot be cut into two disconnected diagrams only by cutting one solid line. For example,

is a connected diagram while
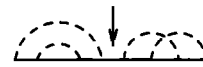
is not since it can be cut into two disconnected parts by cutting a solid line at the position indicated by the arrow. We define

$$\Sigma(k) = O = \underset{k\text{-}q}{\overset{q}{\rule{1.2cm}{0.4pt}}} + \rule{1.2cm}{0.4pt} + \rule{1.2cm}{0.4pt} + \cdots \qquad (17)$$

as the sum over all connected diagrams where k is the external wave number.

Reordering (16), one obtains

$$\rule{2cm}{1.5pt} = \rule{1.5cm}{0.4pt} + \rule{1cm}{0.4pt}\!\!O\!\!\rule{1cm}{1.5pt}$$

which can be divided by $\hat{G}_0(k, \omega) \hat{\mathcal{G}}(k, \omega)$ such that we finally obtain

$$\hat{\mathcal{G}}(k, \omega)^{-1} = \hat{G}_0(k, \omega)^{-1} - \Sigma(k, \omega)$$

$$= i\omega + ik \cdot U + D_{lm} k_l k_m - \Sigma(k, \omega) \qquad (18)$$

In field theory this identity is called the "Dyson equation." It tells us that it is sufficient to calculate the contributions of

connected diagrams if we intend to find the averaged Green's function.

3. Macrodispersion

The asymptotic behavior for large times and distances can be derived by taking the limit for low frequencies and wave numbers. From the Feynman rules and the incompressibility condition

$$\hat{\Delta}_{lm}(\mathbf{q})q_m = 0 \tag{19}$$

following from $\mathbf{k} \cdot \mathbf{u}(\mathbf{k}) = 0$, it is easy to see that $\Sigma(\mathbf{k})$ has the following asymptotic form for $\mathbf{k} \to 0$ and $\omega \to 0$:

$$\Sigma(\mathbf{k}, \omega) = {}^{-}\sigma_{lm}k_lk_m + O(\mathbf{k}^3) \tag{20}$$

with a symmetric tensor σ_{lm}. Hence $\mathscr{G}(\mathbf{k}, \omega)$ behaves asymptotically like

$$\mathscr{G}(\mathbf{k}, \omega) \sim (i\omega + i\mathbf{k} \cdot \mathbf{U} + D_{lm}^*k_lk_m)^{-1} \tag{21}$$

$$\mathbf{k} \to 0 \quad \text{and} \quad \omega \to 0$$

where the macrodispersion coefficient D_{lm}^* is defined as

$$D_{lm}^* := D_{lm} + \sigma_{lm} = D_{lm} - \frac{1}{2}\frac{\partial^2}{\partial k_l\partial k_m}\Sigma(\mathbf{k})\Big|_{\mathbf{k}=0} \tag{22}$$

and the second equality follows from (20).

The simplest possible approximation is to cut the series for Σ in (17) after the first term, i.e., to consider only the one-loop approximation

$$\Sigma^{(1)}(\mathbf{k}) \sim \overset{\frown}{\underset{\rule{2.5em}{0pt}}{\vrule height 0pt depth 0.6em width 0pt}}\!\!\! \tag{23}$$

Evaluating this utilizing the Feynman rules, we obtain

$$\Sigma^{(1)}(\mathbf{k}, \omega) = -\left(\frac{1}{2\pi}\right)^d \int d^dq\, k_lk_m\hat{\Delta}_{lm}(\mathbf{q})G_0(\mathbf{k} - \mathbf{q}, \omega) \tag{24}$$

and from this

$$D_{lm}^* = D_{lm} + \left(\frac{1}{2\pi}\right)^d \int d^dq\, \frac{\Delta_{lm}(\mathbf{q})}{i\omega + i\mathbf{q} \cdot \mathbf{U} + D_{rs}q_rq_s} \tag{25}$$

which coincides with the well-known result of *Gelhar and Axness* [1983].

4. Renormalization Group Analysis

Until now, we have obtained results by averaging the fluctuations over all wave numbers in one single step. However, if the fluctuations are large, this approach may not be justified. In fact, if the covariance function $\Delta_{lm}(\mathbf{x})$ does not decay fast enough for large distances [e.g., *Avellaneda and Majda*, 1992a, b], the right-hand side of (25) becomes infinite. This can indicate anomalous (non-Fickian) transport behavior like that observed by *Matheron and de Marsily* [1980] in the case of a perfectly stratified heterogeneous aquifer, where even for well-behaved covariance functions $\Delta_{lm}(\mathbf{x})$, the second moment of the concentration may increase asymptotically proportional to $t^{3/2}$, leading formally to an infinite value of the effective dispersion coefficient for $t \to \infty$.

A number of interesting results about anomalous scaling have been obtained utilizing a so-called RNG approach. The basic idea is to perform the averages not over all wave numbers in one step but iteratively over (infinitesimal) wave number bands. In this work we present a simplified version for the case of Fickian diffusion. Our starting point is the convection dispersion equation which is averaged in the first step over all contributions with a wave number larger than a large value Λ (i.e., over small-scale fluctuations). Neglecting some higher-order contributions, the averaged equation can be rewritten in the form of the original convection-dispersion equation, however, with smoothed (truncated) fluctuations composed only of the contributions with wave numbers smaller than Λ and a slightly increased ("renormalized") dispersion coefficient. Then this procedure is iterated for a new wave number band $\Lambda - \delta\Lambda < k < \Lambda$, etc., until finally $\Lambda = 0$. At this stage all fluctuations in the velocity field have been averaged out such that only the mean velocity is occurring in the final equation. In the limit $\delta\Lambda \to 0$ one obtains a system of ordinary differential equations describing the change of the diffusion coefficient after averaging over an infinitesimal wave number band.

For the general case of anomalous diffusion it is necessary to "compensate" the reduction of the wave number space due to averaging out small-scale contributions by (If $\mathbf{U} \neq 0$, a coordinate transformation $\mathbf{x} \mapsto \mathbf{x} - \mathbf{U}t$ has to be performed before) rescaling k by an appropriate factor δ. In order to obtain an invariant equation, ω has to be rescaled by a factor $\delta^{2\alpha}$. The value of α is determined by the condition that the resulting averaged equation converges to a nontrivial limit equation for $\Lambda \to 0$ [e.g., *Avellaneda and Majda*, 1992a]. For Fickian diffusion the result is $\alpha = 1$, reflecting the fact that a diffusion equation with constant coefficients remains unchanged under the transformation

$$\begin{aligned} \mathbf{x} &\mapsto \delta^{-1}\mathbf{x} \\ t &\mapsto \delta^{-2}t \end{aligned} \tag{26}$$

We will assume that the resulting behavior is Fickian, such that there is no necessity for performing the rescaling transformations. If this assumption does not hold, our analysis would yield divergent or vanishing values for the macrodispersion coefficient, and the anomalous scaling exponent (if it exists) has to be derived explicitly.

4.1. Infinitesimal Band Elimination

Let us now average (12) over all wave numbers larger than a value Λ which we will let go to ∞ later. Let us denote the average over small scales by $\langle \ \rangle_\Lambda$ and introduce the notation

$$\begin{aligned} \hat{\mathbf{u}}(\mathbf{k}) &= \hat{\mathbf{u}}^<(\mathbf{k}) \qquad k \le \Lambda \\ \hat{\mathbf{u}}(\mathbf{k}) &= \hat{\mathbf{u}}^>(\mathbf{k}) \qquad k > \Lambda \end{aligned} \tag{27}$$

in order to distinguish between small-scale ($\hat{\mathbf{u}}^>$) and large-scale ($\hat{\mathbf{u}}^<$) fluctuations. Their small-scale averages are

$$\langle \hat{\mathbf{u}}^<(\mathbf{k})\rangle_\Lambda = \hat{\mathbf{u}}^<(\mathbf{k}) \tag{28}$$

$$\langle \hat{\mathbf{u}}^>(\mathbf{k})\rangle_\Lambda = 0 \tag{29}$$

Because of our assumptions of statistical homogeneity and the Gaussian distribution of the fluctuations all averages over products can be performed easily. For example, we obtain

$$\langle \hat{u}_l^<(\mathbf{k}_1)\hat{u}_m^>(\mathbf{k}_2)\hat{u}_n^>(\mathbf{k}_3)\rangle_\Lambda = (2\pi)^d\hat{u}_l^<(\mathbf{k}_1)\hat{\Delta}_{mn}(\mathbf{k}_2)\delta(\mathbf{k}_2 + \mathbf{k}_3)$$

$$\langle \hat{u}_l^<(\mathbf{k}_1)\hat{u}_m^<(\mathbf{k}_2)\hat{u}_n^>(\mathbf{k}_3)\rangle_\Lambda = 0 \tag{30}$$

Now in each diagram any line representing **u** is integrated over **k**. Splitting the integral into regions $k > \Lambda$ and $k \le \Lambda$ means that a dashed line in the original equation gives rise to one diagram in which it is interpreted as $u^>$ and another one where it occurs as $u^<$. For example,

$$\text{(diagram)} \quad (31)$$

Taking the average of (12), we obtain after resummation

$$\text{(diagram)} \quad (32)$$

with a renormalized Green's function $G_\Lambda(\mathbf{k}, \omega)$

$$\text{(diagram)} \quad (33)$$

and a renormalized vertex

$$\text{(diagram)} \quad (34)$$

4.2. Scale Dependent Dispersion

Equation (32) is still exact and has a similar form to our original (10). The perturbative part consists now in approximating the renormalized Green's function and vertex such that (32) obtains the form of the original equation, only with a renormalized dispersion tensor, such that the same procedure can be iterated for the next wave number band. This can be done by the following approximations.

First, we neglect vertex renormaliztion; that is, we neglect all but the first term in the calculation of the renormalized vertex. A consistent one-loop calculation would require that we also take into account the second term on the right-hand side of (34). However, in RNG calculations, usually an assumption sometimes called the "distant interaction principle" is exploited, which consists in evaluating all external wave numbers and frequencies (i.e., all wave numbers or frequencies over which no integration is performed) at the point **0**, if this is convenient. This can be regarded as a lowest-order approximation if the integrands are written as a Taylor series around **k** = **0**. In Appendix B we show that the one-loop vertex correction vanishes under this assumption. (This is a peculiarity of incompressible flow: *Dean et al.* [1994] calculated the efficient diffusivity in a gradient (i.e., irrotational) flow and obtained excellent (and probably exact) results by taking one-loop vertex renormalization into account.) To our knowledge, there is no rigorous justification of this approximation. In some cases it leads to remarkably good results, however, *Avellaneda and Majda* [1992a] showed by comparison with a problem allowing an exact RNG treatment that the approximate first-order RNG analysis utilized in this paper may fail to predict the correct scaling behavior for anomalous diffusion.

Second, we observe that (33) has the same form as (16) but with the difference that the integration extends only over wave numbers $q > \Lambda$. With the same arguments as above we find as the one-loop approximation for the renormalized Green's function for $\mathbf{k} \to \mathbf{0}$, $\omega \to 0$

$$G_\Lambda(\mathbf{k}, \omega) \approx \frac{1}{G_0(\mathbf{k}, \omega)^{-1} - \Sigma_\Lambda^{(1)}(\mathbf{k}, \omega)}$$

$$\approx \frac{1}{i\omega + i\mathbf{k} \cdot \mathbf{U} + D_{lm}^*(\Lambda)k_l k_m} \quad (35)$$

which has the required original form with a renormalized dispersion tensor

$$D_{lm}^*(\Lambda) = D_{lm} + \left(\frac{1}{2\pi}\right)^d \int_{q>\Lambda} d^d q \frac{\hat\Delta_{lm}(\mathbf{q})}{i\omega + i\mathbf{q} \cdot \mathbf{U} + D_{rs}q_r q_s} \quad (36)$$

With these two approximations we obtain the original form of the transport equation. To summarize, the effects of the renormalization steps are (1) the random velocity fields consist only of the contributions with wave numbers less than Λ, and (2) the dispersion tensor is changed according to (36). Now we iterate this procedure by averaging this averaged equation over a wave number band $\Lambda - \delta\Lambda < k < \Lambda$. With the same approximations we obtain the original equation again but now with a dispersion tensor

$$D_{lm}^*(\Lambda - \delta\Lambda) = D_{lm}^*(\Lambda)$$

$$+ \left(\frac{1}{2\pi}\right)^d \int_{\Lambda-\delta\Lambda<q<\Lambda} d^d q \frac{\hat\Delta_{lm}(\mathbf{q})}{i\omega + i\mathbf{q} \cdot \mathbf{U} + D_{rs}^*(\Lambda)q_r q_s} \quad (37)$$

The introduction of spherical coordinates in the wave number space and the calculation of the differential coefficient $[D_{lm}^*(\Lambda) - D_{lm}^*(\Lambda - \delta\Lambda)]/\delta\Lambda$ for $\delta\Lambda \to 0$ can be rewritten as a differential equation for $D_{lm}^*(\Lambda)$:

$$\frac{dD_{lm}^*(\Lambda)}{d\Lambda} = -\left(\frac{1}{2\pi}\right)^d \Lambda^{d-1} \int_{q=\Lambda} d\Omega \frac{\hat\Delta_{lm}(\mathbf{q})}{i\omega + i\mathbf{q} \cdot \mathbf{U} + D_{rs}^*(\Lambda)q_r q_s} \quad (38)$$

where the integral on the right-hand side extends over a sphere in the wave number space with center **0** and radius $q = \Lambda$.

By iterating this procedure by successive integration over lower and lower wave number bands, we will finally reach $\Lambda = 0$ such that all fluctuations are averaged out and $D_{lm}^*(\Lambda = 0)$ is the macrodispersion coefficient. Therefore we have to solve the ordinary differential equation (equation (38)) for the initial condition

$$D_{lm}^*(\Lambda = \infty) = D_{lm} \quad (39)$$

in order to find the solution at $\Lambda = 0$.
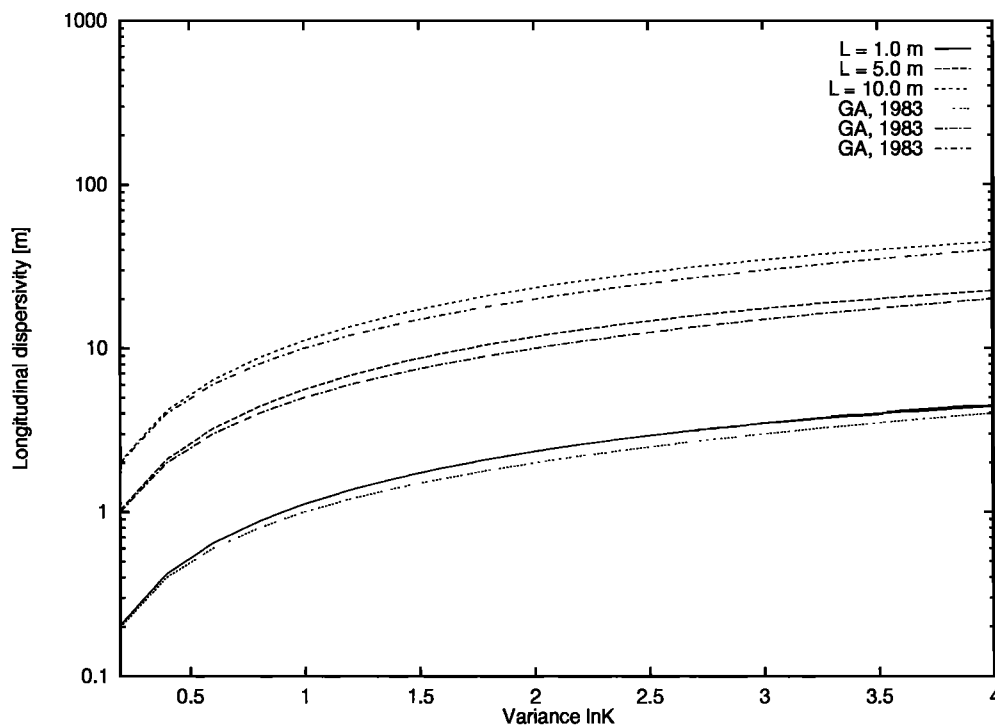
5. Numerical Solution of the RNG Equations

Since the integration of the system (equation (38)) backward in the wave number scale Λ from ∞ to 0 is not so convenient, we reformulate it for a spatial scale $\beta := \Lambda^{-1}$:

$$\frac{dD_{lm}^*(\beta)}{d\beta} = \left(\frac{1}{2\pi}\right)^d \beta^{-d-1} \int_{q=\beta^{-1}} d\Omega \frac{\hat\Delta_{lm}(\mathbf{q})}{i\omega + i\mathbf{q} \cdot \mathbf{U} + D_{rs}^*(\beta)q_r q_s} \quad (40)$$

with the initial condition

$$D_{lm}^*(\beta = 0) = D_{lm} \quad (41)$$

We assume that the mean flow velocity **U** is parallel to the x axis, i.e.,

Figure 1. First-order perturbation theory [*Gelhar and Axness*, 1983] (GA) and RNG values for longitudinal macrodispersivity versus σ_Y^2 for the 3-D isotropic case with correlation lengths $L = 1$, 5, and 10 m.

$$\mathbf{U} = \begin{pmatrix} U \\ 0 \\ 0 \end{pmatrix}$$

As a model for the covariance function of the velocity fluctuations, we used the result from a first-order perturbation theory [*Gelhar and Axness*, 1983; *Dagan*, 1987] for fluctuations in a statistically homogeneous medium with a random permeability field:

$$\hat{A}_{lm}(\mathbf{k}) = U^2\left(\delta_{l1} - \frac{k_1 k_l}{k^2}\right)\left(\delta_{m1} - \frac{k_1 k_m}{k^2}\right)\hat{C}_Y(\mathbf{k}) \qquad (42)$$

where $\hat{C}_Y(\mathbf{k})$ is the Fourier transform of the covariance function $C_Y(\Delta\mathbf{x})$ of the logarithm of the permeability K:

$$C_Y(\Delta\mathbf{x}) := \langle Y(\mathbf{x} + \Delta\mathbf{x})Y(\mathbf{x})\rangle = \langle \ln K(\mathbf{x} + \Delta\mathbf{x}) \ln K(\mathbf{x})\rangle \qquad (43)$$

For C_Y we chose an anisotropic function with exponential decay:

$$C_Y(\mathbf{x}) = \sigma_Y^2 \exp\left[-(x^2/L_x^2 + y^2/L_y^2 + z^2/L_z^2)^{1/2}\right] \qquad (44)$$

where σ_Y^2 is the variance of ln K and L_x, L_y, and L_z are correlation lengths in the x, y, and z directions.

The system of coupled ordinary differential equations (ODEs) resulting from the application of the RNG method was solved numerically. A fifth-order Runge Kutta method with adaptive step size control was used for the set of equations describing the 2-D and 3-D cases [*Press et al.*, 1992]. The integration interval for the ODEs ranged between 0 and 1000. This was enough for all calculations to reach asymptotic behavior.

The integrals occurring at the right-hand side were solved using Gaussian quadrature. The integrals for the 2-D case were solved using the Numerical Algorithms Group Library (NA-Glib) routine d01ahf based on Patterson's method (for the 2-D case with exponentially decaying C_Y defined in (44) the resulting integrals can also be calculated analytically). Integration was performed up to a relative accuracy of 10^{-7}. The double integrals for the 3-D case were solved with a similar method also due to Patterson (NAGlib d01daf). Integrals were evaluated up to an accuracy of 10^{-7}. Improved accuracy was obtained by exploiting the symmetry of the integrand. For the 3-D case this implies a change of the integration intervals from $[0, \pi] \times [0, 2\pi]$ to $[0, \pi/2] \times [0, \pi/2]$, and the integral was multiplied by 8. For the 2-D case the interval was changed from $[0, 2\pi]$ to $[0, \pi]$, and the integral was multiplied by 4. In order to handle the steep variation of the integrand occurring at θ, where θ is the angle between q and U and equal to $\pi/2$, the integration interval was split into two intervals ranging from 0 to 1.565 and from 1.565 to $\pi/2$. The choice of the value 1.565 was based on visual inspection of the integrand. For other parameter sets, splitting into a larger number of subregions or an adaptive method may be necessary. Another approach is to subtract the integrand with θ set to $\pi/2$ (i.e., subtract the close to singular part) leading to a two-dimensional integral with a harmless integrand and a one-dimensional integral which can be solved analytically. Comparison of both methods for various test cases showed the same results. In the subsequent discussion, the first procedure was applied for all calculations.

The quality of the numerical approach and the consistency of the program were evaluated by comparison with the *Gelhar and Axness* [1983] (GA) macrodispersion values for a statistically isotropic medium. The GA values are obtained by simply fixing the dispersivities at the right-hand sides at their local value. Eight cases were analyzed with a constant dispersivity value ($D_{11} = D_{22} = D_{33}$). The differences were less than 1%
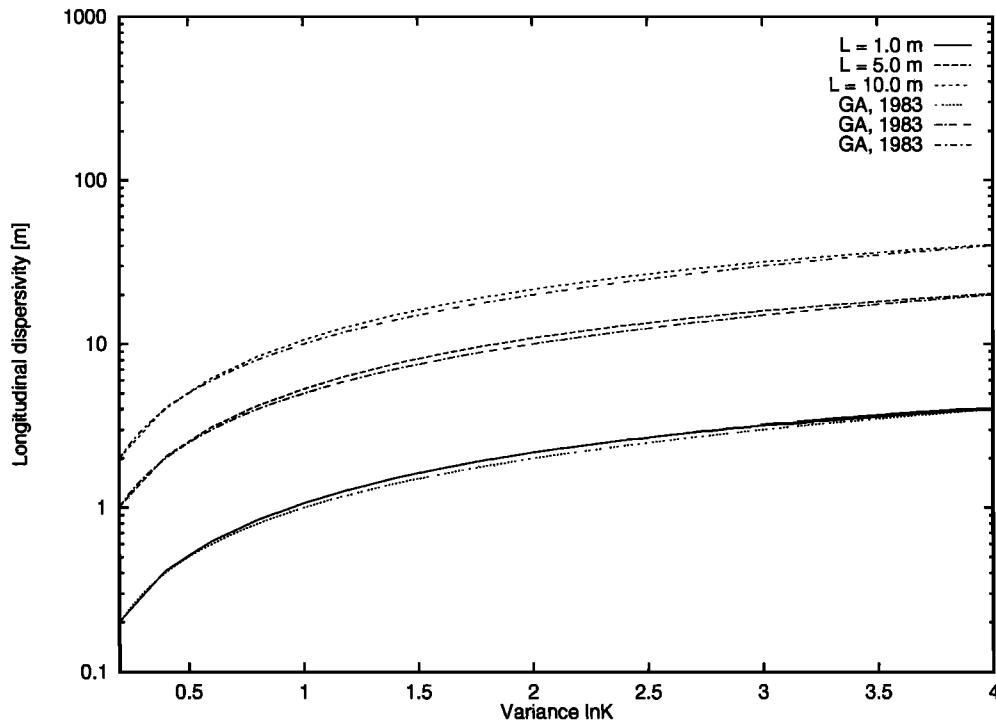
Figure 2. GA and RNG values for longitudinal macrodispersivity versus σ_Y^2 for the 2-D isotropic case with correlation length $L = 1$, 5, and 10 m.

between the calculated values and the approximations of GA. Similar results were obtained for the 2-D case.

We then calculated the macrodispersion values using renormalization and compared them with the results obtained by the theory of GA. Calculations were performed for a statistically isotropic medium with local dispersivity values equal to 0.001 and three different correlation scales of the hydraulic conductivity K. Figure 1 shows the results obtained for the longitudinal and transverse dispersivities for various values of the variance of the log transformed K in three dimensions. Evaluating the longitudinal dispersivity, good agreement is found between both approaches especially for small variances (<0.4). As the variance becomes larger, differences increase slightly with higher values obtained for the renormalization approach. Results for the 2-D cases are shown in Figures 2 and 3. Similar results are obtained in two dimensions. However, the deviations are somewhat smaller for the 2-D case compared to the 3-D case.

Large differences between both theories are found for the transverse dispersivity. For the 3-D case this is shown in Figure 4. Renormalization results in transverse dispersivities which are much larger than the ones obtained by GA. In addition, they are dependent upon the correlation length of the hydraulic conductivity. The larger the correlation length, the larger the transverse dispersivities become. For $L = 1.0$ and small variances, transverse dispersivities are about 50 times larger than the ones obtained by GA. This increases up to a factor of 100 for large variances. A similar effect is found for the transverse dispersivities in the 2-D case. In general, the values obtained from RNG in the 2-D case are larger than for the 3-D case. This corresponds to the general finding that effective dispersivities calculated from a 2-D stochastic theory are larger than the values obtained from a 3-D theory.

While the first-order perturbation theory predicts that the

transverse dispersion is proportional to the local value of the dispersion coefficient D (GA) we observed that the RNG prediction for higher variances is practically independent of this value. An example is shown in Figure 4. This agrees well with the result of Monte Carlo simulations presented in the next section.

6. Comparison With Numerical Simulations

Like most perturbative approaches to the macrodispersion problem our analysis rests on several approximations whose validity is difficult to prove. In order to check the validity we performed some Monte Carlo simulations for the three-dimensional case with

$$\hat{C}_Y(k) = \lambda(2\pi)^2 \frac{3}{\sqrt{8\pi}} \exp\left(\frac{-k^2}{2}\right) \tag{45}$$

This case of an isotropic bell-shaped covariance function was chosen for convenience; the algorithm described below can be modified easily in order to describe different cases as well.
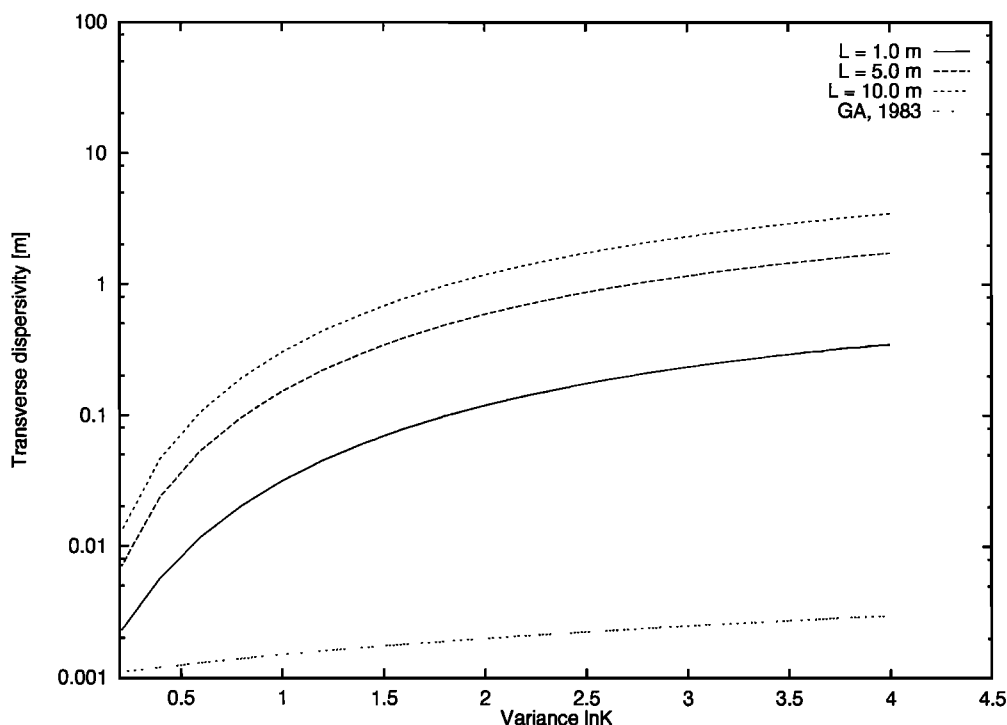
With (42) and (45) one obtains

$$\langle u^2 \rangle = \frac{1}{(2\pi)^3} \int d^3k \hat{\Delta}_{ll}(k) = \lambda U^2 \tag{46}$$

Hence λ is the ratio of the variance of the perturbation and the square of the mean field.

The random fields are generated by a finite number N of sines as

$$u_l(\mathbf{x}) = \sqrt{\frac{3\lambda}{N}} \sum_{i=1}^{N} \sin (\mathbf{k}^{(i)} \cdot \mathbf{x} + \phi^{(i)})\left(\delta_{lm} - \frac{k_l^{(i)}k_m^{(i)}}{k^{(i)2}}\right)U_m \tag{47}$$

Figure 3. GA and RNG values for transverse macrodispersivity versus σ_Y^2 for the 2-D isotropic case with correlation length $L = 1$, 5, and 10 m.

where $\phi^{(i)}$ is a uniformly distributed random phase drawn from the interval $[0, 2\pi]$ and $\mathbf{k}$ is a vector drawn from a 3-D Gaussian distribution with zero mean and unit variance. These random fields are divergence free and fulfill (42) and (45). The results shown in this paper were obtained using $N = 64$ modes; test calculations with a larger number of modes (up to 1000) gave the same results.

An effective dispersion coefficient was determined by releasing a small number n of particles ($n = 4 \cdots 20$) for each realization at the point $\mathbf{x} = \mathbf{0}$, following the propagation of the particles over a time t by a particle-tracking method [e.g., *Thompson and Gelhar*, 1990] and calculating the dispersion coefficient D^*_{ll} along the l axis as

$$D^*_{ll} = \sigma_{ll}/(2t) = \frac{n \sum x_l^{(j)}(t)^2 - [\sum x_l^{(j)}(t)]^2}{2n(n-1)t} \tag{48}$$

where $x_l^{(j)}(t)$ is the l coordinate of the jth particle at time t and σ_{ll} is the unbiased estimate of the variance of the l coordinates. These values are averaged over an ensemble of a number R of realizations ($R = 800 \cdots 2000$), and the error is defined as the usual error of the ensemble-averaged mean.

Figures 5 and 6 show the time dependence of D^* in longitudinal (x) and transverse (y) directions for the case $\lambda = 1$ and $U = 1$. It is interesting to note that the transverse dispersion coefficient reaches its saturation value (or the "Fickian regime") earlier than the longitudinal does. This behavior was also observed in all simulations with different parameters, and it fits to our observation above that the RNG method predicts saturation of the dispersion coefficient in the transverse direction at comparatively small scales as compared to the longitudinal one.

Figure 6 shows that another qualitative feature of the RNG treatment is also confirmed by our simulations: The long-term

transverse macrodispersion coefficient D^*_T does not depend on the value of the local dispersion coefficient D if $D_* \ll |D|$. This is definitely in contradiction to GA's first-order perturbation theory where D^*_T is proportional to the local dispersion.

Quantitatively, Figure 7 shows the dependence of the longitudinal and transverse dispersion coefficient on λ for the case $U = 1$. As one would guess from the small differences of RNG and first-order perturbation theory results for the longitudinal direction, the prediction of the longitudinal dispersion coefficient is very satisfying. In the transverse direction the values determined from the simulations were 30%–50% smaller than those predicted by the RNG approach. Though this error is larger than in the longitudinal direction, the values are much better than the prediction of the first-order perturbation theory. Very similar results were obtained for other choices of U or (equivalently) broader and narrower distributions $C_Y(k)$.

7. Comparison With the Borden Site Field Experiment

It is well documented in literature that both the GA theory and the linear theory of *Dagan* [1989] based on a Lagrangian formulation stochastic solute transport underestimate the effective transverse dispersivities. Except for the quasi-linear theory of *Neuman and Zhang* [1990], none of the approaches presently available is able to calculate transverse dispersivities which are of the order of magnitude of observed data.

We compared our theory with results obtained at the Borden Site natural gradient tracer experiment. Both chloride and bromide were injected, and their spatial and temporal spreading monitored for a 3 year period. Using a three-dimensional covariance model to describe the spatial variability of the hydraulic conductivity, *Sudicky* [1986] estimated the variance to
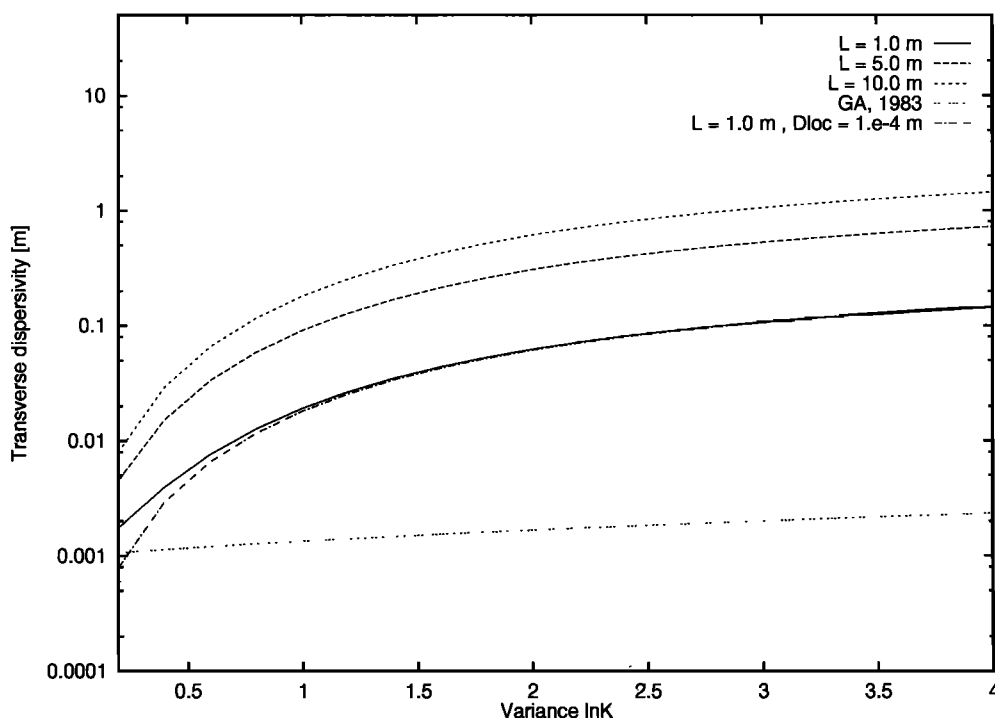
Figure 4. First-order perturbation theory (GA) and RNG values for transverse macrodispersivity versus σ_Y^2 for the 3-D isotropic case with correlation lengths $L = 1$, 5, and 10 m. Note that GA predicts that the transverse dispersivity does not depend on L. For $L = 1$ m, results are shown for two different values of the local dispersion coefficient, $D = 10^{-3}$ m^2 d^{-1} (solid curve) and $D = 10^{-4}$ m^2 d^{-1} (dash-dotted curve). Unlike that predicted by GA, the renormalized coefficient does not depend crucially on D for the long term.

be equal to 0.29 with a horizontal isotropic correlation length of about 2.8 m and a vertical one equal to 0.12 m. The mean velocity of the groundwater is 0.09 m/d based on the horizontal velocity of the center of the mass of the plume. *Freyberg* [1986] calculated the spatial moments of the depth-averaged plume. By fitting straight lines to the centered second-order spatial moments Freyberg calculated effective longitudinal and transverse dispersivities of 0.36 and 0.039, respectively. These calculations were based on a time period of 647 days. It is worthwhile noting that according to Freyberg, asymptotic conditions were not reached indicating that the effective values might be somewhat larger. Using the three-dimensional stochastic transport theory of GA, a longitudinal macrodispersivity of 0.6 m was obtained. The transverse components of the macrodispersivity were orders of magnitude smaller than the observed values. Using the two-dimensional linear theory of *Dagan* [e.g., 1987, 1989], Freyberg obtained a value equal to 0.49 m for the longitudinal dispersivity and calibrated values for the variance of the hydraulic conductivity (0.24) and the horizontal correlation length (2.7 m). Using a quasi-linear theory, *Neuman and Zhang* [1990] and *Zhang and Neuman* [1990] obtained a value of 0.51 m for the longitudinal dispersivity and 0.0095 for the transverse dispersivity (including local dispersion). In their comparison the effective Peclet number was defined on the basis of the effective longitudinal dispersivity. By placing more emphasis on the late data point for the second-order moment a longitudinal dispersivity of 0.4 m was assumed. This value was then used to calculate the effective Peclet number, and from this, using the quasi-linear theory, the effective dispersivities were obtained.

Figures 8 and 9 show the results obtained with our theory for

the 2-D and 3-D cases. Calculations were done using a value of 0.0052 for the local dispersivity in the longitudinal direction and 0.002 for the transverse dispersivity. These estimates were also used by *Zhang and Neuman* [1990] in their comparison with the Borden data. The longitudinal dispersivity is about 0.87 m which is substantially larger than the 0.36 m. A better agreement is found for the transverse dispersivity where a value of 0.032 is obtained, which is close to the value estimated at the Borden Site. Applying the 3-D approach, setting the vertical local dispersivity equal to the horizontal one, and accounting for anisotropy, we obtain 0.41 and 0.023 for the longitudinal and transverse dispersivities. Unfortunately, no 3-D spatial moments are available for comparison. In any case the values obtained with the 3-D model are in perfect agreement with the dispersivities obtained from the spatial 2-D moments. In addition, we are able to calculate transverse dispersivities which are of order of magnitude of those obtained from measurements.

8. Summary and Conclusions

Existing linear perturbation theories describing large-scale behavior of solutes in heterogeneous aquifers are known to underestimate asymptotic values of the transverse dispersivities. In this paper we presented an approximate renormalization group method which calculates the asymptotic values of the macrodispersion tensor.

A diagrammatic perturbation expansion for the averaged Green's function for the convection dispersion equation was developed. In the one-loop approximation of this expansion we recovered the equations derived by *Gelhar and Axness* [1983].
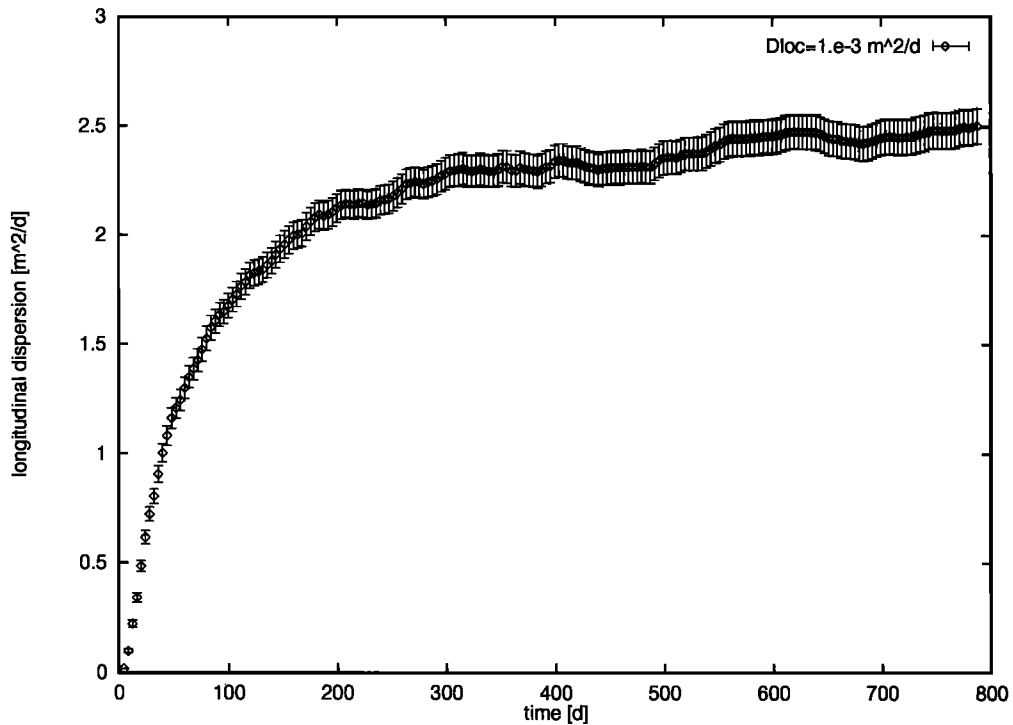
Figure 5. Time dependence of the effective longitudinal dispersion in a 3-D Monte Carlo simulation for $\lambda = 1$ and $U = 1$.
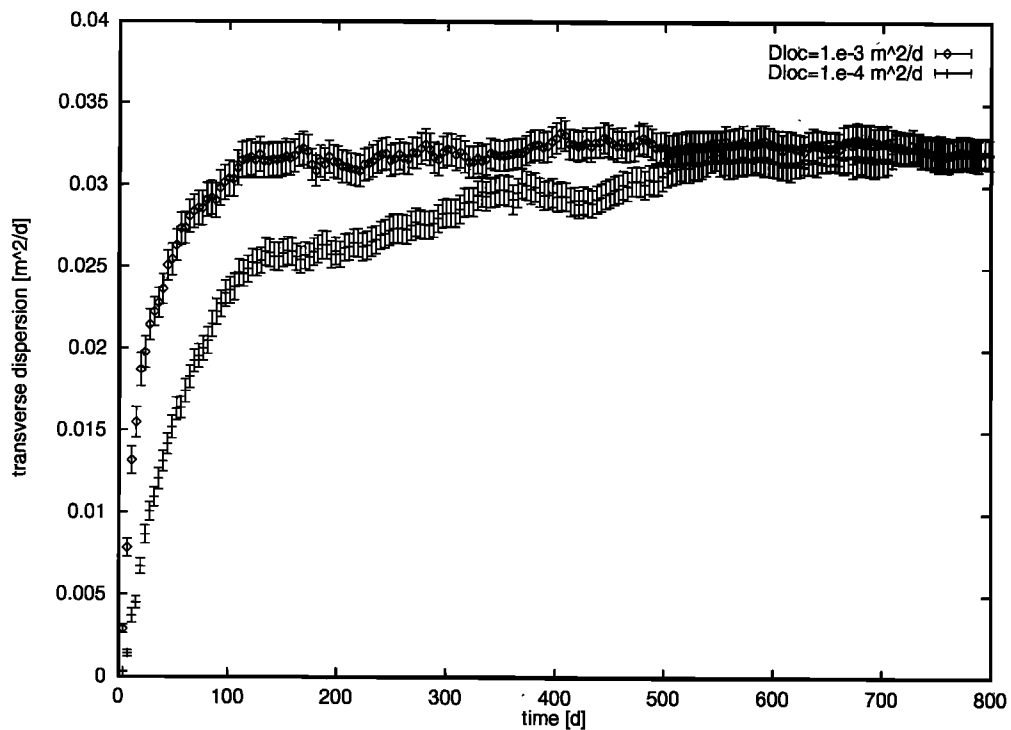
Figure 6. Time dependence of the effective transverse dispersion in a 3-D Monte Carlo simulation for $\lambda = 1$, $U = 1$, and two different values of the local dispersivity. Unlike first-order perturbation theory, both the renormalization group (RNG) prediction and the Monte Carlo simulation yield a transverse dispersivity practically independent of the small local value for the long term.
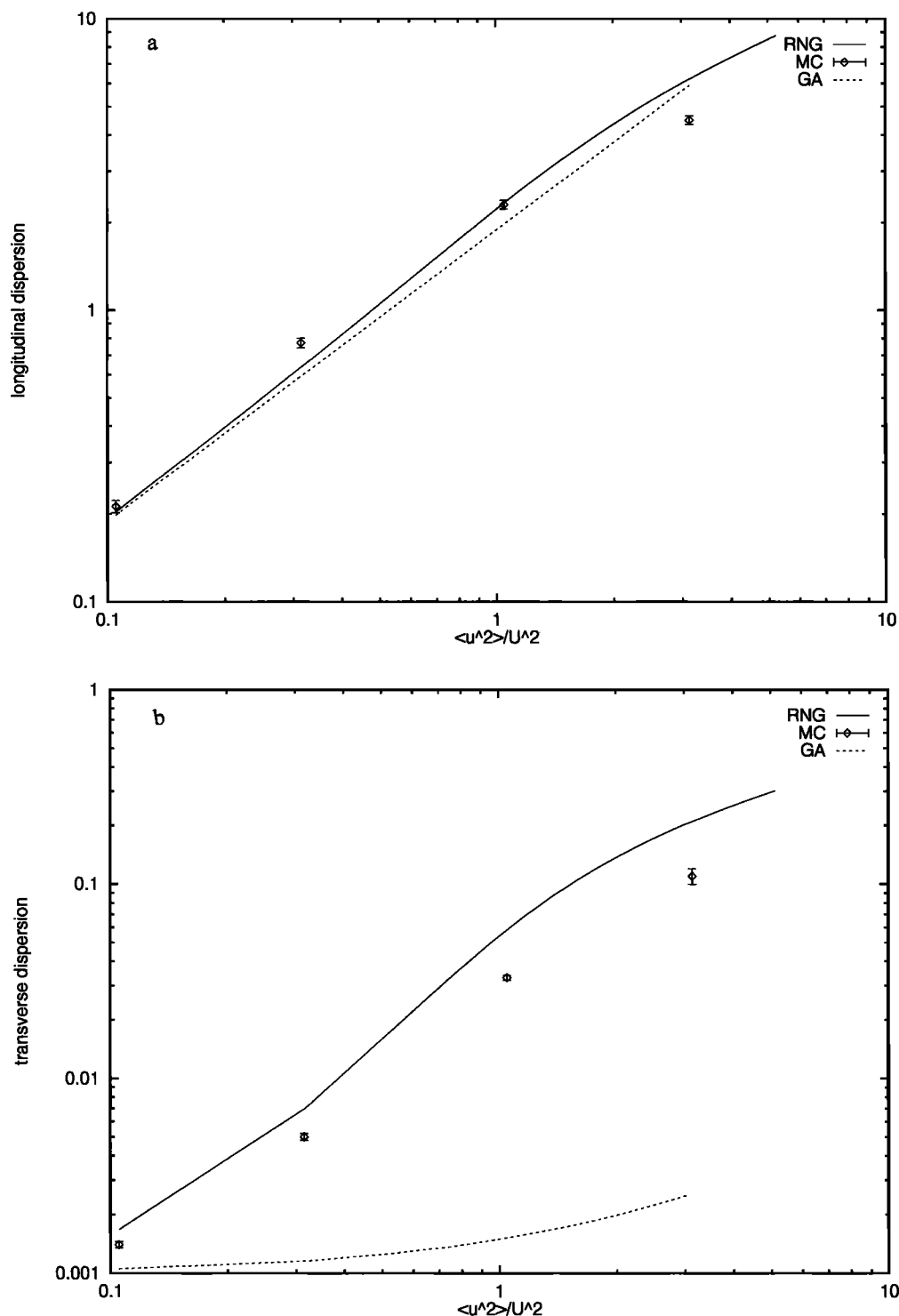
Figure 7. Dependence of the effective (a) longitudinal and (b) transverse dispersion coefficient on $\lambda = \langle u^2 \rangle / U^2$. RNG is the RNG prediction; MC is the Monte Carlo simulation; and GA is the first-order perturbation theory.

Alternatively to this classical perturbation theory, we applied an approximate renormalization group method resulting in a coupled system of ordinary differential equations for a scale dependent dispersion tensor. The large-scale limit of the solution provides an approximation for the macrodispersion tensor.

Compared to the results of Gelhar and Axness [1985], the RNG treatment gave only small corrections to the effective

longitudinal dispersivity. For reasonable strengths of the fluctuations, we expect these corrections to be smaller than the experimental error in the field experiments. The values for the transverse components, however, were increased by several orders of magnitude. Additionally, we observed that the value of the renormalized transverse dispersivity depends on the correlation length, which is not the case in Gelhar and Axness' theory.
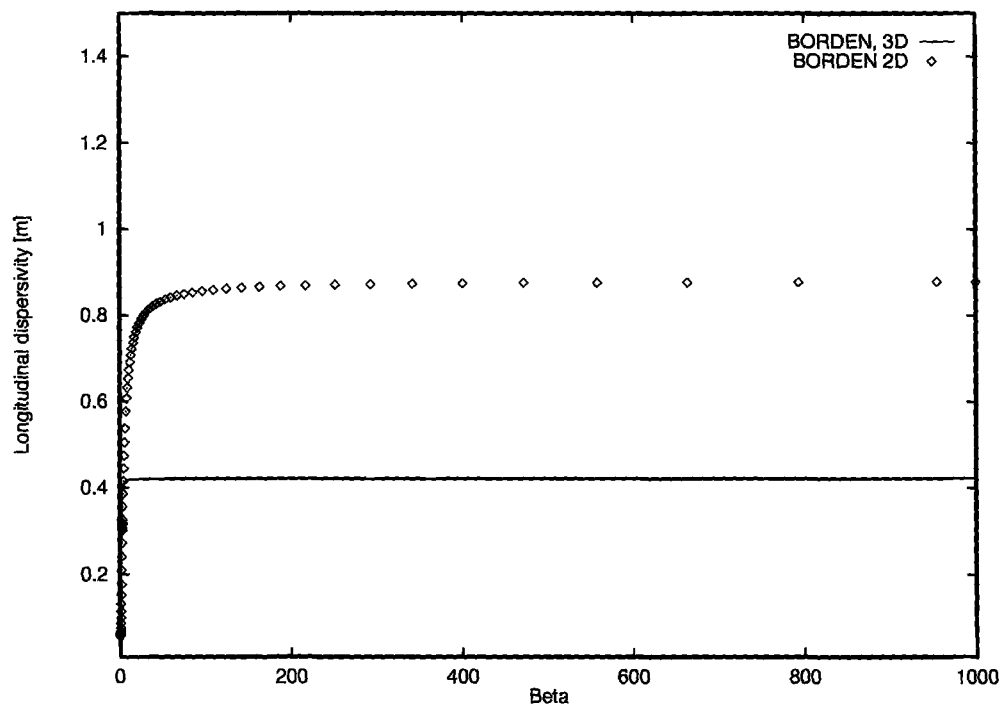
Figure 8. The 2-D and 3-D scale dependence of the longitudinal dispersivity for the Borden Site.

The results were compared to the outcome of Monte Carlo simulations, and we observed good qualitative agreement between predictions of the RNG analysis and the numerical experiments. The long-term dispersivity predicted by the RNG treatment was not exact but overestimated by a factor of about 2 at the most. This, however, is much closer than the prediction of the first-order perturbation theory which may be off by several orders of magnitude. A comparison with reported data from the Borden Site field experiment showed a good agreement between our RNG calculations and observed dispersivities. The RNG approach may also be very suited to treat a large class of problems showing anomalous diffusion properties.
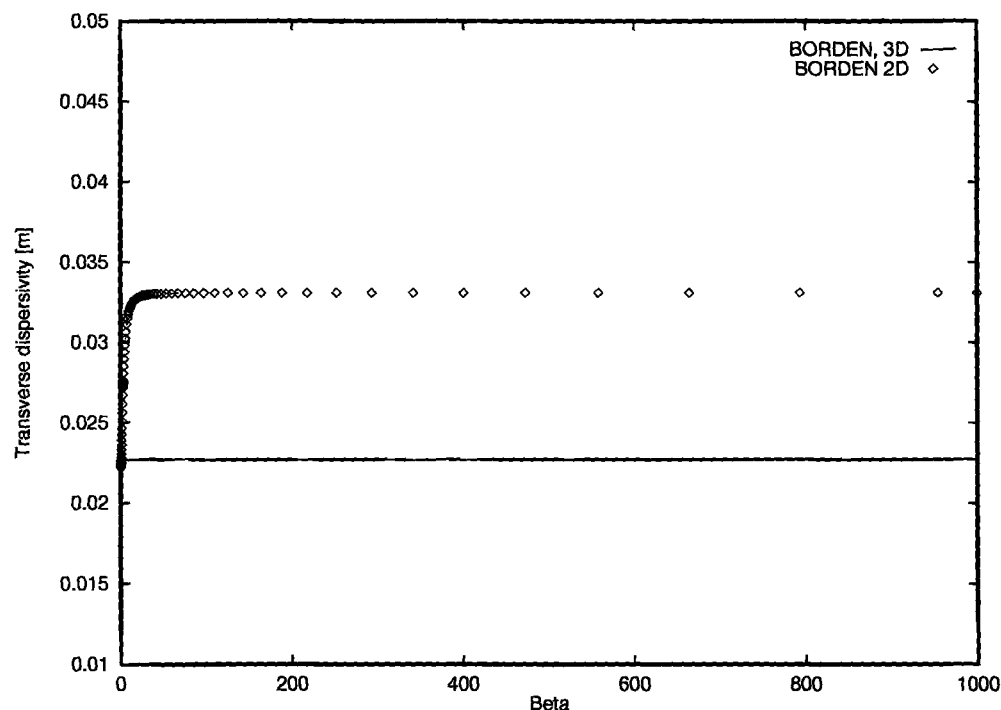

Figure 9. The 2-D and 3-D scale dependence of the transverse dispersivity for the Borden Site.

Appendix A: Fourier Transform Conventions

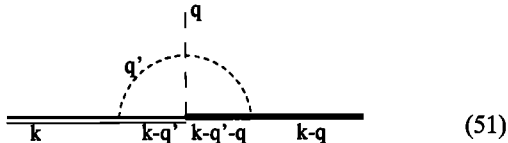We define the Fourier transform $\hat{f}$ of a function f on a d-dimensional space as

$$\hat{f}(\mathbf{k}) := \int d^d x \, \exp\,(-i\mathbf{k}\cdot\mathbf{x})f(\mathbf{x}) \tag{49}$$

The inverse operation is then determined by

$$f(\mathbf{x}) = \frac{1}{(2\pi)^d}\int d^d k \, \exp\,(i\mathbf{k}\cdot\mathbf{x})\hat{f}(\mathbf{k}) \tag{50}$$

Appendix B: Vertex Renormalization

In order to find the one-loop vertex correction we have to evaluate the following diagram $D(1)$:

$$\tag{51}$$

The rule for a vertex in the original equation is to integrate over $\mathbf{q}$ the expression

$$\hat{u}_l(\mathbf{q})(k_l - q_l) =: \Gamma_{lm}u_l(\mathbf{q})(k_m - q_m) \tag{52}$$

with $\Gamma_{lm} = \delta_{lm}$. We introduced a tensor Γ_{lm} since we shall see immediately that vertex renormalization with a scalar correction is not possible.

With the Feynman rules and (19) we evaluate the diagram above as

$$D(1) = \int d^d q \int_{q'>\Lambda} d^d q' \, G_A(\mathbf{k})G_A(\mathbf{k}-\mathbf{q}')G(\mathbf{k}-\mathbf{q}-\mathbf{q}')$$

$$\cdot \, G(\mathbf{k}-\mathbf{q})\Delta_{lm}(\mathbf{q}')k_l(k_m - q_m)u_r(\mathbf{q})(k_r - q_r') \tag{53}$$

A tensorial vertex correction $\delta\Gamma_{lm}$ should lead to a term of the form

$$\int d^d q \, G_A(\mathbf{k})G(\mathbf{k}-\mathbf{q})\delta\Gamma_{lm}u_l(\mathbf{q})(k_m - q_m)$$

and by comparing with (53) and renaming the indices m and r, we see that

$$\delta\Gamma_{lm} = \int_{q'>\Lambda} d^d q' \, G_A(\mathbf{k}-\mathbf{q}')G(\mathbf{k}-\mathbf{q}-\mathbf{q}')\Delta_{mr}(\mathbf{q}')k_r(k_l - q_l') \tag{54}$$

which, in general, cannot be expressed introducing a scalar correction $\delta\Gamma$. The correction depends on $\mathbf{k}$ and $\mathbf{q}$. If we assume $\mathbf{k} = \mathbf{q} = 0$ according to the distant interaction principle, i.e., neglect higher-order terms in $\mathbf{k}$ and $\mathbf{q}$, we obtain $\delta\Gamma_{lm} = 0$.

Note that we used the incompressibility condition from (19). If $\Delta_{lm}(\mathbf{q})q_l \neq 0$, the integrand would contain nonvanishing terms proportional to $\Delta_{lr}(\mathbf{q}')q_m'q_r'$.

References

Avellaneda, M., and A. J. Majda, Approximate and exact renormalization theories for a model of turbulent transport, *Phys. Fluids A, 4,* 41–57, 1992a.

Avellaneda, M., and A. J. Majda, Mathematical models with exact renormalization for turbulent transport, II, Fractal interfaces, non-Gaussian statistics, and the sweeping effect, *Commun. Math. Phys., 146,* 139–205, 1992b.

Bouchaud, J.-P., and A. Georges, Anomalous diffusion in disordered media: Statistical mechanisms, models, and physical applications, *Phys. Rep., 195,* 127–293, 1990.

Christakos, G., D. T. Hristopulos, and C. T. Miller, Stochastic diagrammatic analysis of groundwater flow in heterogeneous porous media, *Water Resour. Res., 31*(7), 1687–1703, 1995.

Dagan, G., Theory of solute transport by groundwater, *Ann. Rev. Fluid Mech., 18,* 183–215, 1987.

Dagan, G., *Flow and Transport in Porous Media,* 465 pp., Springer-Verlag, New York, 1989.

Dean, D. S., I. T. Drummond, and R. R. Horgan, Perturbation schemes for flow in random media, *J. Phys. A Math Gen., 27,* 5135–5144, 1994.

Deem, M. W., and D. Chandler, Classical diffusion in strong random media, *J. Stat. Phys., 76,* 911–927, 1994.

Feynman, R. P., Space-time approach to nonrelativistic quantum mechanics, *Rev. Mod. Phys., 20,* 367–387, 1948.

Freyberg, D. L., A natural gradient experiment on solute transport in a sand aquifer, 2, Spatial moments and the advection and dispersion of nonreactive tracers, *Water Resour. Res., 22*(13), 2047–2058, 1986.

Gelhar, L. W., and C. L. Axness, Three-dimensional stochastic analysis of macrodispersion in aquifers, *Water Resour. Res., 19*(1), 161–180, 1983.

King, P. R., The use of field theoretic methods for the study of flow in a heterogeneous porous medium, *J. Phys. A Math Gen., 20,* 3935–3947, 1987.

Kraichnan, R. H., Dynamics of nonlinear stochastic systems, *J. Math. Phys. N. Y., 2,* 124–148, 1961.

LeBlanc, D. R., S. P. Garabedian, K. M. Hess, L. W. Gelhar, R. D. Quadri, K. G. Stollennwerk, and W. W. Wood, Large-scale natural gradient tracer test in sand and gravel, Cape Cod, Massachusetts, 1, Experimental design and observed tracer movement, *Water Resour. Res., 27*(5), 895–910, 1991.

Matheron, G., and G. de Marsily, Is transport in porous media always diffusive? A counter example, *Water Resour. Res., 16,* 901–917, 1980.

Neuman, S. P., and Y. K. Zhang, A quasi-linear theory of non-Fickian and Fickian subsurface dispersion, 1, Theoretical analysis with application to isotropic media, *Water Resour. Res., 26*(5), 887–902, 1990.

Phythian, R., and W. D. Curtis, The effective long-time diffusivity for a passive scalar in a Gaussian model fluid flow, *J. Fluid Mech., 89,* Part 2, 241–250, 1978.

Press, W. H., A. S. Teukolsky, W. T. Vetterling, and B. P. Flannery, *Numerical Recipes in FORTRAN,* 963 pp., Cambridge Univ. Press, New York, 1992.

Sudicky, E. A., A natural gradient experiment on solute transport in a sand aquifer: Spatial variability of hydraulic conductivity and its role in the dispersion process, *Water Resour. Res., 22,* 13: 2069–2082, 1986.

Tompson, A. F. B., and L. W. Gelhar, Numerical simulation of solute transport in three-dimensional, randomly heterogeneous porous media, *Water Resour. Res., 26*(10), 2541–2562, 1990.

Wilson, K. G., and J. Kogut, The renormalization group and the ε expansion, *Phys. Rep., 12,* 75–100, 1974.

Yakhot, V., and S. A. Orszag, Renormalization group analysis of turbulence, I, Basic theory, *J. Sci. Comput., 1,* 3–51, 1986.

Zhang, Q., Transient behavior of mixing induced by a random velocity field, *Water Resour. Res., 31*(3), 577–591, 1995.

Zhang, Y. K., and S. P. Neuman, A quasi-linear theory of non-Fickian and Fickian subsurface dispersion, 2, Application to anisotropic media and the Borden Site, *Water Resour. Res., 26*(5), 903–913, 1990.

U. Jaekel, Institute of Chemistry and Dynamics of the Geosphere ICG-4, Research Center Jülich, D-52425 Jülich, Federal Republic of Germany. (e-mail: u.jackel@fz-juelich.de)

H. Vereecken, Institute of Petroleum and Organic Chemistry, ICG-4, Forschungszentrum Julich GmbH, Leo Brand Strasse, 52425 Julich, Federal Republic of Germany. (e-mail: h.vereecken@fz-juelich.de)